CHAPTER X

ACTIVE INFRARED THERMOGRAPHY TECHNIQUES FOR THE NONDESTRUCTIVE TESTING OF MATERIALS

Clemente Ibarra-Castanedo[1], Marc Genest[2], Jean-Marc Piau[1], Stéphane Guibert[1], Abdelhakim Bendada[1] and Xavier P. V. Maldague[1]

[1]Computer Vision and Systems Laboratory, Laval University, Quebec City (Quebec) G1K7P4, Canada .E-mails: {IbarraC, JMPiau, Guibert, Bendada, MaldaguX}@gel.ulaval.ca

[2] Institute for Aerospace Research (IAR), National Research Council Canada (NRC), 1200 Montreal Road, Bldg. M-14, Room 130, Ottawa, ON, Canada, K1A 0R6. E-mail: Marc.Genest@nrc-cnrc.gc.ca

Active infrared thermography refers to the group of methods employed to inspect the integrity of materials or systems through the use of an external energy source and an infrared detector. The external stimulus can be of many forms such as warm or cold air, heat pulses, periodic thermal waves, or mechanical oscillations, *e.g.* ultrasounds. The way data is captured and processed, as well as the typical applications differ according to the excitation source. This chapter presents a review of three of the most common active techniques in the field of thermography: pulsed thermography, lock-in thermography and vibrothermography.

1. Introduction

Infrared (IR) thermography is a nondestructive testing (NDT) technique, *i.e.* an inspection method for the examination of a part, material or system without impairing its future usefulness [1]. When compared with other classical NDT techniques such as C-Scan ultrasonics or X-Rays, data acquisition by infrared thermography is safe, nonintrusive and noncontact, allowing the detection of relatively shallow subsurface defects (a few millimeters in depth) under large surfaces (typically 30x30 cm^2 at once, although inspection of larger surfaces is possible) and in a fast manner (from a fraction of a second to a few minutes depending in the configuration, see below). Any object above the absolute zero temperature will emit IR radiation. Infrared radiation corresponds to the band of the electromagnetic

spectrum between 0.74 and 1000 μm. Hence, an excellent way to measure thermal variations is to use an IR radiometer, usually a focal plane array (FPA) camera capable of detecting radiation in the mid (3 to 5 μm) or long (8 to 14 μm) wave infrared bands, denoted as MWIR and LWIR, respectively, corresponding to two of the high transmittance atmospheric windows as shown in Figure 1.

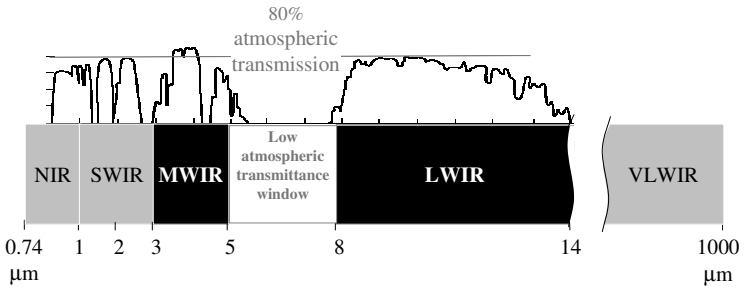

Figure 1: The infrared bands in the electromagnetic spectrum.

There are two approaches in infrared thermography as seen in Figure 2: (1) *passive*, in which the features of interest are naturally at a higher or lower temperature than the background, *e.g.* surveillance of people on a scene; and (2) *active*, in which an energy source is required to produce a thermal contrast between the feature of interest and the background, *e.g.* a specimen with internal flaws.

The active approach is adopted in many cases given that the inspected parts are usually in equilibrium with the surroundings.

A wide variety of energy sources can be used to induce a thermal contrast between defective and non-defective zones that can be divided in *external*, if the energy is delivered to the surface and then propagated through the material until it encounters a flaw; or *internal*, if the energy is injected into the specimen in order to stimulate exclusively the defects. Typically, external excitation is performed with optical devices such as photographic flashes (for heat pulsed stimulation) or halogen lamps (for periodic heating), whereas internal excitation can be achieved by means of mechanical oscillations, with a sonic or ultrasonic transducer for both burst and amplitude modulated stimulation.

As depicted in Figure 2, there are three classical active thermographic techniques based on these two excitation modes: lock-in thermography and pulsed thermography, which are optical techniques applied externally; and vibrothermography, which uses ultrasonic waves (amplitude modulated or

pulses) to excite internal features. Lock-in thermography is presented first.

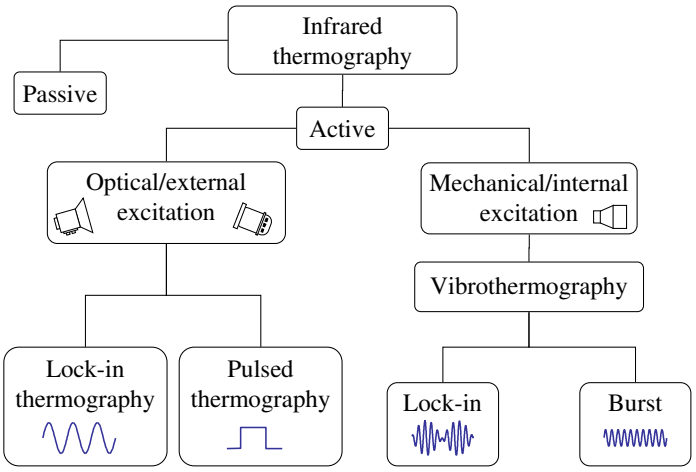

Figure 2: Infrared thermography approaches.

2. Lock-in thermography

2.1. Basic theory for lock-in thermography

Lock-in thermography (LT) also known as *modulated thermography* [2] is a technique derived from *photothermal radiometry* [3], in which, a small surface spot is periodically illuminated by an intensity modulated laser beam to inject thermal waves into the specimen. The thermal response is recorded at the same time using an infrared detector and decomposed by a lock-in amplifier to extract the amplitude and phase of the modulation [4]. Photothermal radiometry was a raster point-by point technique that required long acquisition times (especially in the case of deep defects involving very low modulation frequencies, see below). Furthermore, extra hardware, *i.e.* lock-in amplifier, is needed in order to retrieve the amplitude and phase of the response.

Fortunately, it is possible to dramatically simplify and speed up the acquisition process for NDT applications by replacing: (1) the laser beam with one or several modulated heating sources, *e.g.* halogen lamps, that cover the entire specimen surface instead of only a point; (2) the infrared detector with an infrared camera capable of monitoring the whole (or a large part of the) surface (typically in a 320x256 or 640x512 pixel matrix configuration);

and (3) the lock-in hardware with a software capable of recovering mathematically the amplitude and phase of the response. This is what is called lock-in thermography [5].

Sinusoidal waves are typically used in LT, although other periodic waveforms are possible. Using sinusoids as input has the advantage that the frequency and shape of the response are preserved; only the amplitude and phase delay of the wave may change (*i.e.* sinusoidal fidelity). The periodic wave propagates by radiation through the air until it touches the specimen surface where heat is produced and propagates through the material. Internal defects act as barrier for heat propagation, which produces changes in amplitude and phase of the response signal at the surface.

Heat diffusion through a solid is a complex 3D problem that can be described by the Fourier's law of heat diffusion (or the heat equation) [6]:

$$\nabla^2 T - \frac{1}{\alpha} \cdot \frac{\partial T}{\partial t} = 0 \tag{1}$$

where $\alpha = k/\rho c_P$ [m^2/s] is the thermal diffusivity of the material being inspected, k [W/mK] its thermal conductivity, ρ [kg/m^3] its density and c_P [J/kgK] its specific heat at constant pressure.

The Fourier's law 1D solution for a periodic thermal wave propagating through a semi-infinite homogeneous material may be expressed as [7]:

$$T(z,t) = T_o \exp(-\frac{z}{\mu}) \cos\left(\frac{2\pi \cdot z}{\lambda} - \omega t\right) \tag{2}$$

where T_0 [°C] is the initial change in temperature produced by the heat source, $\omega = 2\pi f$ [rad/s] is the modulation frequency, f [Hz] is the frequency, $\lambda \equiv 2\pi\mu$ [m] is the thermal wavelength; and μ [m] is the thermal diffusion length, which determines the rate of decay of the thermal wave as it penetrates through the material and is defined by [7]:

$$\mu \equiv \sqrt{\frac{2 \cdot \alpha}{\omega}} = \sqrt{\frac{\alpha}{\pi \cdot f}} \tag{3}$$

Figure 3 depicts a thermal wave as it travels from the surface through a solid. As can be seen, after the waveform travels only a distance equal to a thermal diffusion length μ, it has been already reduced to 1/535 its initial intensity. From Eq. (3), in order to cover a distance equal to a thermal wavelength λ, a thermal wave at f=10 Hz will be able to travel less than 0.4 mm through

plastic, slightly more than 11 mm through aluminum (see Figure 3) and almost 16 mm through air. Hence, thermal waves propagate deeper in more diffusive materials. On the other hand, information about deeper features is available when lower frequencies are used.

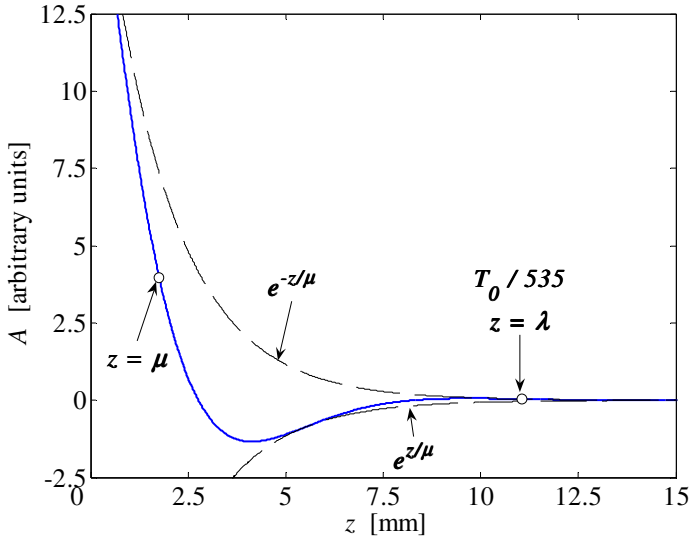

Figure 3. Thermal wave propagation by conduction through an aluminum semi-infinite plate at 10 Hz.

These two aspects are important to know when planning the inspection of a part in order to correctly select the working frequency and to determine the depth of internal defects as will be pointed out in section 2.3. The next paragraph describes the experimental setup and the acquisition system in more detail.

2.2. Experimental setup and data acquisition for lock-in experiments

Figure 4 depicts a lock-in thermography experiment. Two lamps are shown although it is possible to use several lamps mounted on a frame to reduce the non-uniform heating and/or to increase the amount of energy delivered to the surface. The lamps send periodic waves (*e.g.* sinusoids) at a given modulation frequency ω, for at least one cycle, ideally until a steady state is achieved, which depends on the specimen's thermal properties and the defect depth, see Eq. (3) above. In practice however, only a few cycles are needed to adequately retrieve phase and amplitude data, much before attaining steady state conditions.

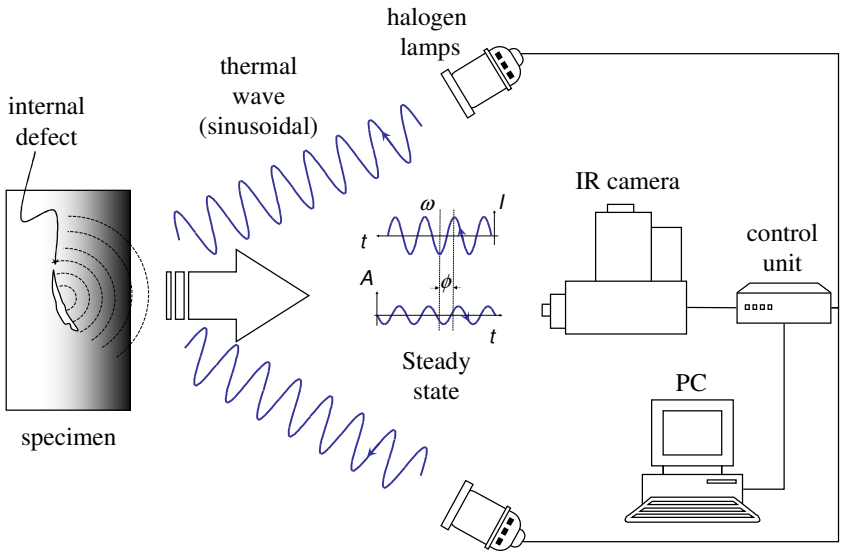

Figure 4. Experimental set-up for lock-in thermography.

Figure 5 shows an example of the raw output signal for a sinusoidal input at two different points. As can be seen, noise is omnipresent and processing is required not only to extract the amplitude and/or phase information but also to de-noise the signal.

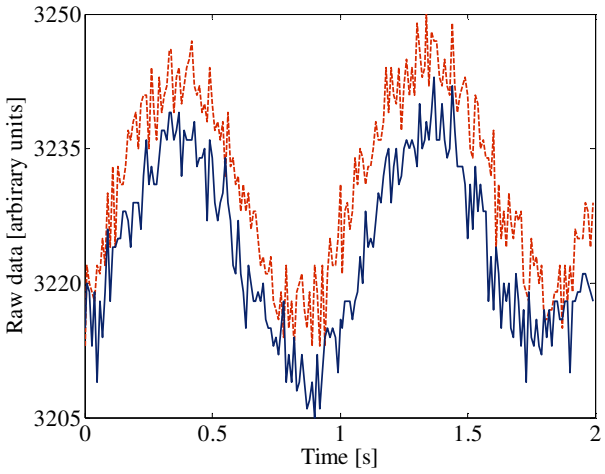

Figure 5: Raw data output signal at f=1 Hz for 4 different points.

In the following paragraph, we present two processing techniques for LT.

2.3. Processing lock-in thermography data

A four point methodology for sinusoidal stimulation is available [5], [8] and illustrated in Figure 6.

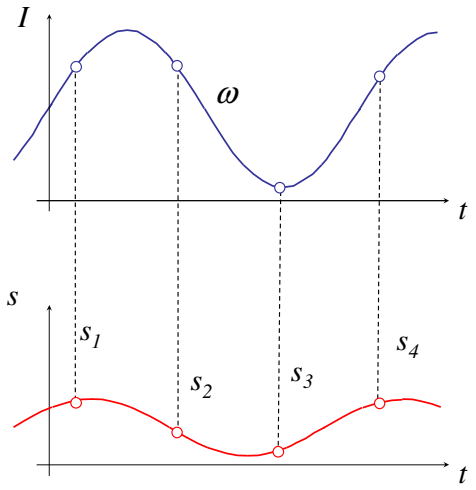

Figure 6: Four point methodology for amplitude and phase delay estimation by lock-in thermography.

The sinusoidal input signal *I*, is represented on top of Figure 6, the response signal *S* is depicted at the bottom. As mentioned before, input and output have the same shape when sinusoids are used, there is only a change in amplitude and phase that can be calculated as follows [8]:

$$A = \sqrt{(S_1 - S_3)^2 + (S_2 - S_4)^2} \tag{4}$$

$$\phi = \arctan\left(\frac{S_1 - S_3}{S_2 - S_4}\right) \tag{5}$$

The 4-point method is fast but it is valid only for sinusoidal stimulation and is affected by noise. The signal can be de-noised in part by averaging of several points instead of a single one and/or by increasing the number of cycles. Another possibility is to fit the experimental data using least squares regression [9] and to use this synthetic data to calculate the amplitude and the phase. This two alternatives contribute to slow down the calculations. Alternatively, the discrete Fourier transform (DFT) can be used to extract amplitude and phase information from LT data. Initially proposed for pulsed

thermography data [10] (see pulsed phase thermography below), the DFT can be written as [11]:

$$F_n = \Delta t \sum_{k=0}^{N-1} T(k\Delta t)\exp^{(-j2\pi nk/N)} = \mathrm{Re}_n + \mathrm{Im}_n \tag{6}$$

where j is the imaginary number (j^2=-1), n designates the frequency increment (n=0,1,…N); Δt is the sampling interval; and *Re* and *Im* are the real and the imaginary parts of the transform, respectively.

In this case, real and imaginary parts of the complex transform are used to estimate the amplitude and the phase [10]:

$$A_n = \sqrt{\mathrm{Re}_n^2 + \mathrm{Im}_n^2} \tag{7}$$

$$\phi_n = \tan^{-1}\left(\frac{\mathrm{Im}_n}{\mathrm{Re}_n}\right) \tag{8}$$

The DFT can be use with *any* waveform (even transient signals as in pulsed phase thermography and burst phase vibrothermography, see below) and has the advantage of de-noising the signal. Although very useful, Eq. (6) is slow. Fortunately, the fast Fourier transform (FFT) algorithm is available [12] to be implemented or can be found (integrally or simplified) in common software packages.

One of the most interesting characteristics of LT testing is the possibility of performing quantitative operations in a straightforward manner. As discussed at the end of section 2.1, a direct relationship exists between the depth of a defect and the thermal diffusion length, μ [13], *i.e.* Eq. (3). For instance, empirical expressions have been proposed [14], [15] to extract the depth of a given defect from LT data using a relationship of the form:

$$z = C_1 \cdot \mu = C_1 \cdot \sqrt{\frac{\alpha}{\pi \cdot f_b}} \tag{9}$$

where f_b is known as the blind frequency [16], *i.e.* the frequency at which a given defect have enough (phase or amplitude) contrast to be detected (at frequencies higher than f_b is not possible to detect it), C_1 is an empirical constant.

It has been observed that, C_1=1 when using amplitude data [13], whilst reported values when working with the phase are in the range $1.5<C_1<2$ [13]-

[17], with C_1=1.82 typically adopted [14], [15] following the research work by Thomas et al., 1980 [18]. The phase is therefore of more interest in NDT than the amplitude, since it provides deeper probing capabilities. Moreover, the ratio involved in Eqs. (5) and (8), cancels part of the artifacts related to non-uniform heating, environmental reflections, emissivity variations and surface geometry variations.

2.4. Advantages, disadvantages and applications

Given that LT requires to perform an experiment for each and every inspected depth and there is a stabilization time before reaching a permanent regime, inspection by lock-in thermography is in general slower than other approaches such as pulsed thermography, which will be described in the following section. A complete LT experiment is carried out by inspecting the specimen at several frequencies, covering a wide range from low to high frequencies, and then a fitting function can be used to complete the amplitude or phase profiles for each point (*i.e.* each pixel). Nevertheless, there exists a direct relationship between depth and the inspection frequency that allows depth estimations to be performed from amplitude or phase data without further processing. Furthermore, the energy required to perform an LT experiment is generally less than in other active techniques, which might be interesting if a low power source is to be used or if special care has to be given to the inspected part, *e.g.* cultural heritage pieces, works of art, frescoes, etc. [19].

Some typical applications include determination of coatings thickness, detection of delaminations, determination of local fiber orientation, corrosion detection and inspection of cultural properties. [4], [19].

3. Pulsed thermography

3.1. Basic theory for pulsed thermography

In pulsed thermography (PT), the specimen surface is submitted to a heat pulse using a high power source such as photographic flashes. A heat pulse can be though as the combination several periodic waves at different frequencies and amplitudes. After the thermal front come into contact with the specimen's surface, a thermal front travels from the surface through the specimen. As time elapses, the surface temperature will decrease *uniformly* for a piece without internal flaws. On the contrary, subsurface discontinuities (*e.g.* porosity, delaminations, disbonds, fiber breakage, inclusions, etc.), can

be though as resistances to heat flow that produce abnormal temperature patterns at the surface, which can be detected with an IR camera.

The 1D solution of the Fourier equation for the propagation of a *Dirac* heat pulse, *i.e.* an ideal waveform defined as an intense unit-area pulse of so brief duration that no measuring equipment is capable of distinguishing it from even shorter pulses [11], in a semi-infinite isotropic solid by conduction has the form [6]:

$$T(z,t) = T_0 + \frac{Q}{\sqrt{k\rho c_P \pi t}} \exp(-\frac{z^2}{4\alpha t}) \tag{10}$$

where Q [J/m^2] is the energy absorbed by the surface and T_0 [K] is the initial temperature.

A Dirac heat pulse is composed of periodic waves at *all* frequencies and amplitudes. Although it is not possible to reproduce such a waveform in practice, a heat pulse provided by a powerful source such as a photographic flash having approximately a square shape, can be used. In this case, the signal is composed by periodic waves at *several* (but not all) frequencies. The shorter the pulse, the broader the range of frequencies. This is very useful for understanding the link between lock-in and pulse thermography, which give rise to pulsed phase thermography that will be discussed in paragraph 3.3.

From Eq. (10), the thermal profiles for an aluminum specimen subjected to a uniform heat pulse follows the behavior portrayed in Figure 7.

The profiles correspond to 4 depths: z=0, 0.05, 0.1 and 0.25 mm. Thermal evolution for deep defects starts at zero and reaches peak intensity at a given time (longer for deeper defects) and then slowly decays approximately as the square root of time. Shallower defects show higher peak intensities earlier. At the surface the behavior is somehow different starting at a high temperature and monotonically decaying following approximately the square root of time. At the surface (z=0 mm), Eq. (10) can be rewritten as follows:

$$T(0,t) = T_0 + \frac{Q}{e\sqrt{\pi t}} \tag{11}$$

where $e \equiv (k\rho c_P)^{1/2}$ [m] is the effusivity, which is a thermal property that measures the material ability to exchange heat with its surroundings.

Although Eq. (11) is only an approximation of the complex 3D diffusion problem described by Fourier's law, *i.e.* Eq. (1), many of the processing techniques have been based on this simplification to perform qualitative and

quantitative analysis, as will be discussed in paragraph 3.3. The experimental setup is discussed first.

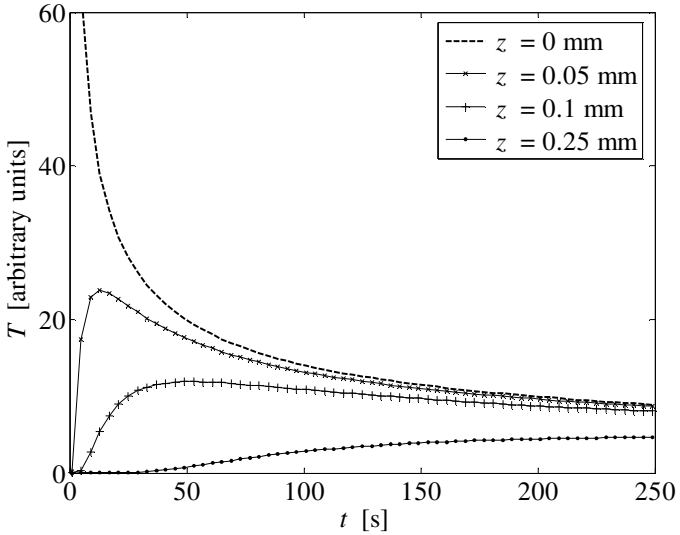

Figure 7. Thermal profiles at four depths (z=0, 0.05, 0.1 and 0.25 mm) for an aluminum plate subjected to a uniform heat pulse.

3.2. Experimental setup and data acquisition for pulsed thermography

When compared to LT, data acquisition in PT is fast and straightforward as illustrated in Figure 8.

Two photographic flashes are used to heat up the specimen's surface, after what, the thermal changes are recorded with an infrared camera. A synchronization unit is needed to control the time between the launch of the thermal pulse and the recording with the IR camera. Data is stored as a 3D matrix (see Figure 9a) where x and y are the spatial coordinates, and t is the time. Temperature decreases approximately as $t^{1/2}$ (at least at early times), as predicted by Eq. (11), except for the defective areas, where the cooling rate is different (see Figure 9b).

Although heat diffusion is a complex problem, the relationship between defect depth and time, simplified through Eq. (11), has been exploited by many researchers to develop qualitative and quantitative techniques. Next section presents three techniques that are used to analyze PT data. These techniques were considered to be some of the most promising ones among many others and they are currently subjected to extensive investigation.

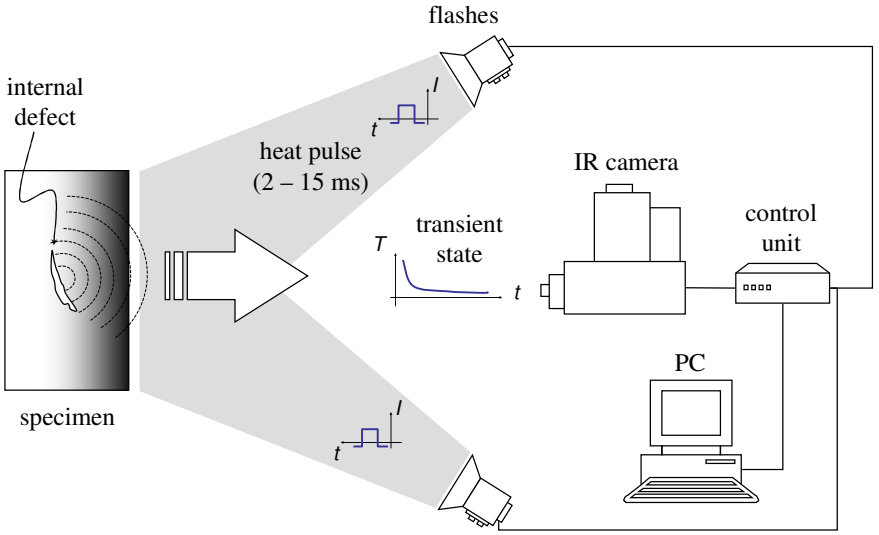

Figure 8. Experimental set-up for pulsed thermography.

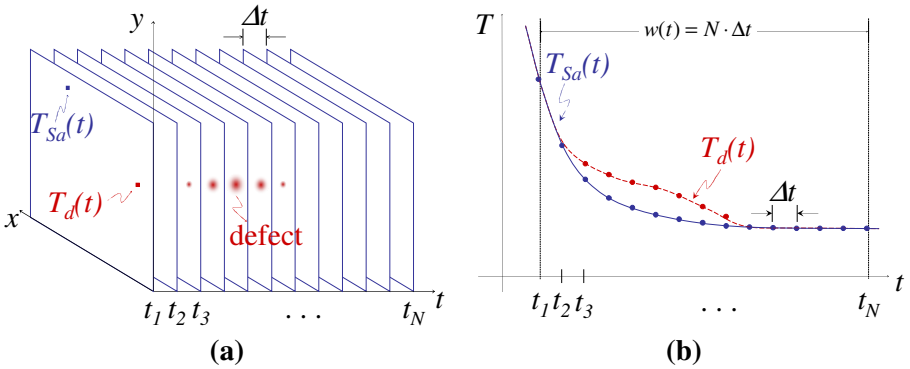

Figure 9. Temperature evolution: (a) data 3D matrix, and (b) temperature profile for a defective (dotted line) and non-defective (continuous line) pixels.

3.3. Processing pulsed thermography data

PT is probably the most extensively investigated approach because of its ease of deployment. Raw PT data however, is difficult to handle and analyze. There are a great variety of processing techniques that have being developed to enhance the subtle IR signatures [10], [20], [21]. Space being limited, it is only possible to discuss a few of them. We selected three techniques that

have shown very promising results for most common applications. Although only a brief discussion is provided; interested readers may consult the references provided below.

3.3.1. Thermal contrast based techniques

Thermal contrast is a basic operation that despite its simplicity is at the origin of most of the PT analysis. Various thermal contrast definitions exist [22] p. 198, but they all share the need to specify a sound area S_a, *i.e.* a non-defective region within the field of view. For instance, the *absolute* thermal contrast $\Delta T(t)$ is defined as [22]:

$$\Delta T(t) = T_d(t) - T_{S_a}(t) \tag{12}$$

with $T(t)$ being the temperature at time t, $T_d(t)$ the temperature of a pixel or the average value of a group of pixels, and $T_{Sa}(t)$ the temperature at time t for the S_a. No defect can be detected at a particular t if $\Delta T(t)$=0.

The main drawback of classical thermal contrast is establishing S_a, especially if automated analysis is needed. Even when S_a definition is straightforward, considerable variations on the results are observed when changing the location of S_a as is well-known [23].

In the *differential absolute contrast* (DAC) method [24], instead of looking for a non-defective area, an ideal S_a temperature at time t is computed locally assuming that on the first few images (at least one image at time t' in particular, see below) this local point behaves as a S_a in accordance to Eq. (11), *i.e.* there is no defect visible. The first step is to define t' as a given time value between the instant when the pulse has been launched t_0, and the precise moment when the first defective spot appears on the thermogram sequence, *i.e.* when there is enough contrast for the defect to be detected, t_1. At t', there is no indication of the existence of a defective zone yet, therefore the local temperature for a S_a is exactly the same as for a defective area [25]:

$$T_{S_a}(t') = T(t') = \frac{Q}{e\sqrt{\pi t'}} \quad \Rightarrow \quad \frac{Q}{e} = \sqrt{\pi t'} \cdot T(t') \tag{13}$$

From this result, T_{Sa} can be computed for every pixel at time t. Substituting Eq. (13) into the absolute contrast definition, *i.e.* Eq. (12), it follows that [25]:

$$\Delta T_{dac} = T(t) - \sqrt{\frac{t'}{t}} \cdot T(t') \tag{14}$$

Actual measurements diverge from the solution provided by Eq. (14) as time elapses and also as plate thickness enlarges with respect to the non-semi-infinite case. Nevertheless, it has proven to be very efficient in reducing artifacts from non-uniform heating and surface geometry [20], and to provide a good approximation even for the case of anisotropic materials [20] at early times. Originally, proper selection of *t'* required an iterative graphical procedure, for which a graphical user interface was developed [26]. An automated algorithm is now available [27]. Furthermore, a modified DAC technique has been developed as well [28]. It is based on a finite plate model, which includes the plate thickness *L* explicitly in the solution, extending in this way the validity of the DAC algorithm to later times.

3.3.2. Pulsed phase thermography

Pulsed phase thermography (PPT) [10], [29] is another interesting technique, in which data is transformed from the time domain to the frequency spectra using the one-dimensional discrete Fourier transform (DFT), *i.e.* Eq. (6). The use of the DFT, or more precisely the FFT on thermographic data was first proposed by Maldague and Marinetti in 1996 [10]. Since then, it has been applied to other thermographic data, such as lock-in, described in section 2 and for vibrothermography data as will be described in section 4. As for the case of LT, the amplitude and the phase can be computed from Eqs. (7) and (8). The frequency components can be derived from the time spectra as follows:

$$f = \frac{n}{N \cdot \Delta t} \tag{15}$$

where designates the frequency increment (n=0,1,…N), Δt is the time step and N is the total number of frames in the sequence.

Phase ϕ is of particular interest in NDE given that it is less affected than raw thermal data by environmental reflections, emissivity variations, non-uniform heating, surface geometry and orientation. These phase characteristics are very attractive not only for qualitative inspections but also for quantitative characterization of materials. For instance, a depth inversion technique using the phase from PPT and Eq. (9) is available [30].

The FFT is typically used to extract amplitude and phase information.

Nevertheless, it is also possible to used different transformation algorithms such as the wavelet transform [31]. The later has the additional advantages of preserving the temporal information after the transformation and to use *wavelets* as the basis function instead of sinusoids. Wavelets are periodic waves of short duration that allow to better reproduce a transient signal and to used different scales or resolutions [32]. These advantages of the wavelet transform are currently under investigation.

3.3.3. Thermographic Signal Reconstruction

Thermographic signal reconstruction (TSR) [33] is an attractive technique that allows increasing spatial and temporal resolution of a sequence, reducing at the same time the amount of data to be manipulated. TSR is based on the assumption that, temperature profiles for non-defective pixels should follow the decay curve given by the one-dimensional solution of the Fourier Equation, *i.e.* Eq. (2), which may be rewritten in the logarithmic form as:

$$\ln(\Delta T) = \ln\left(\frac{Q}{e}\right) - \frac{1}{2}\ln(\pi t) \tag{16}$$

Next, an *n*-degree polynomial is fitted for each pixel [33]:

$$\ln(\Delta T) = a_0 + a_1 \ln(t) + a_2 \ln^2(t) + ... + a_p \ln^p(t) \tag{17}$$

Typically, n is set to 4 or 5 to avoid "ringing" and to insure a good correspondence between data and fitted values. Synthetic data processing brings interesting advantages such as: significant noise reduction, possibility for analytical computations, considerably less storage is required since the whole data set is reduced from N to p+1 images (one per polynomial coefficient), and calculation of first and second time derivatives from the synthetic coefficients is straightforward.

3.4. Advantages, disadvantages and applications

Pulsed thermography is fast (from a few seconds for high conductivity materials to a few minutes for low conductivity materials) and easy to deploy. There are numerous processing techniques available although many of them are complex when compared to lock-in. Thermal based techniques are affected by non-uniform heating, emissivity variations, environmental reflections and surface geometry. These problems however, are dramatically reduced using advanced processing algorithms, *e.g.* PPT, DAC and TSR. For

instance PPT allows the recovering of amplitude and phase data as in LT with the advantage that, since a heat pulse can be seen as a set of several periodic thermal waves launched at once, several data points (amplitude or phase) can be extracted from a single experiment. Nevertheless, as described in [34], special care must be given to the selection of the sampling and truncation parameters in order to perform quantitative calculations by PPT.

4. Vibrothermography

4.1. Basic theory for vibrothermography

Vibrothermography (VT), also known as *ultrasound thermography* [35] or *thermosonics* [36], utilizes mechanical waves to directly stimulate internal defects and without heating the surface as in optical methods (*e.g* LT and PT). If we though of optical lock-in thermography to be the successor of photothermal radiometry as mentioned before, vibrothermography can be seen as the successor of *optoacoustics* or *photoacoustics* [13], [37], [38], in which microphones or piezoceramics in contact with the specimen and a lock-in amplifier were used to detect the thermal wave signature from a defect. This was performed in a point-by-point manner and lack of practical interest at the time. The theory behind however, was the base for the later development of VT.

In the classical ultrasound C-scan NDT inspection, a transducer is placed in contact with the sample with the help of a coupling media. The ultrasonic waves travel through the specimen and are transmitted back to the surface where the transducer pick-up the reflected signal (pulsed-echo technique), or they are collected on the opposite side (transmission). In any case, the principle of defect detection is based on the differences in specific acoustic impedances (Z) between materials. In VT, ultrasonic waves will travel freely through a homogeneous material, whereas an internal defect will produce a complex combination of absorption, scattering, beam spreading and dispersion of the waves, whose principal manifestation will be in the form of heat. Heat then will travel by conduction in all directions, an IR camera can be directed to one of the surfaces of the specimen to capture the defect signature. Ultrasonic waves are ideal for NDT since they are not audible to humans (although some low frequencies harmonics are present), defect detection is independent from of its orientation inside the specimen, and both internal and open surface defects can be detected. Hence, VT is very useful for the detection of cracks and delaminations.

Sonic waves, audible for humans, vibrate between 20 Hz and 20 kHz. The

range for ultrasonic waves, no audible to humans, is between 20 kHz and 1 MHz, although most transducers operate between 15 and 50 kHz. Unlike electromagnetic waves, mechanical elastic waves such as sonic and ultrasonic waves do not propagate in a vacuum; on the contrary, they require a medium to travel. They travel faster in solids and liquids than through the air. This brings about an important aspect of VT: although contactless (through air) ultrasonics is currently under intense investigation in many areas [39], the common approach in VT is to use a coupling media such as a piece of fabric, water-based gels or aluminum, between the transducer and the specimen to reduce losses.

The next paragraph describes the experimental setup for a VT experiment.

4.2. Experimental setup and data acquisition for vibrothermography

There are basically two configurations for VT that can be sought as analog to optical methods described above. The first one is lock-in vibrothermography (or amplitude modulated VT), analog to the LT approach; and the second technique is burst vibrothermography, which is analog to PT. These two approaches are illustrated in Figure 10 and Figure 11.

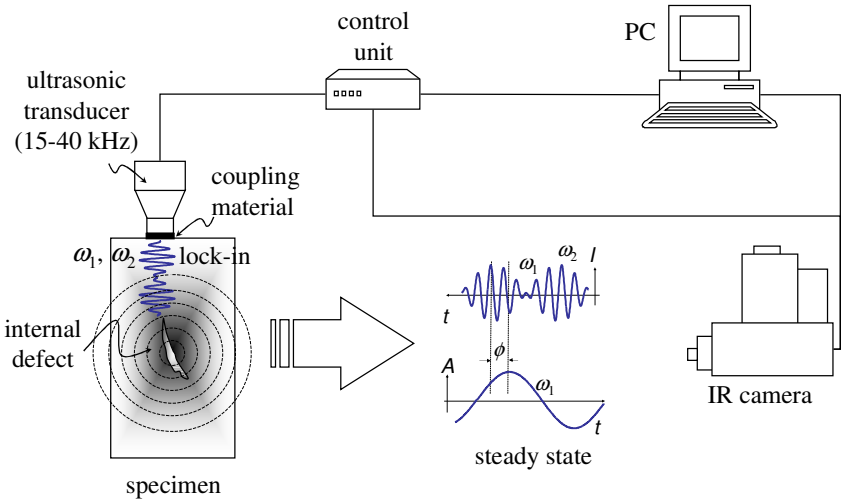

Figure 10. Configuration for lock-in vibrothermography.

It should be mentioned that is also possible to modulate the frequency either in lock-in or burst VT [40]. This approach is sometimes called *wobbulation*. The idea is to cover a range of ultrasonic frequencies, instead of only one,

since it is not always possible to predict the right frequency for a particular application. Ultrasonic wobbulation can be compared to a heat pulse, which is composed of thermal waves at many frequencies. Wobbulation is useful as well to prevent the appearance of *standing waves*, which are produced when working at the natural harmonics resonance frequency of the material. In practice however, it is sometimes preferable to repeat the acquisition at a different frequency since the commercial transducers commonly used are not suitable for frequency modulations.

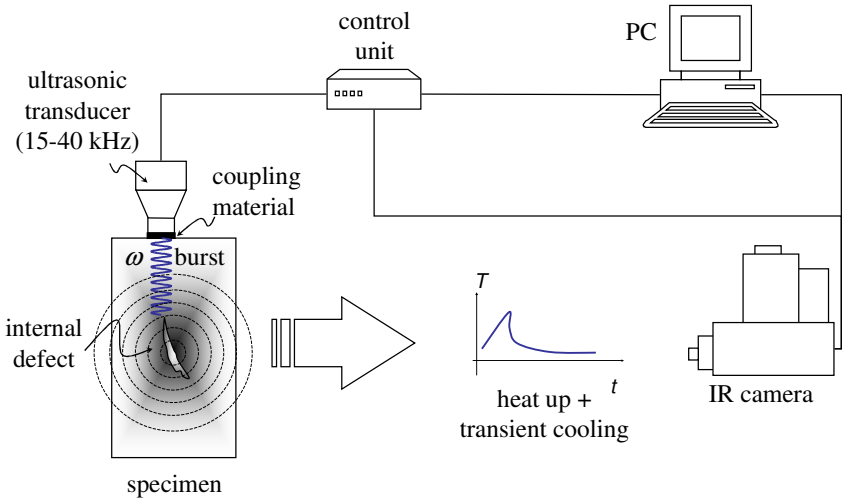

Figure 11. Configuration for burst vibrothermography.

The ultrasound wave is produced by a transducer made of a stack of piezo elements and concentrated in a titanium horn that acts like a hammer. Hence, the part being inspected should be firmly immobilized (but without damaging) to avoid cantilever effects, clapping and sliding of the transducer. The transducer horn should be pressed against the sample as well to improve the coupling transmission of the ultrasound into the specimen. Insertion of a material between the transducer and the sample is strongly recommended not only as a coupling medium, but also to avoid damage of the sample and correct misalignment. A bad coupling implies a poor ultrasound transmission but more seriously it creates unwanted heat in the vicinity of the ultrasound injection point.

After the elastic waves are injected to the specimen, they travel through the material and dissipate their energy mostly at the defects so heat is locally released. The thermal waves then travel by conduction to the surface, where they can be detected with an IR camera.

When compared to optical/external techniques, the thermal wave travels half the distance in a VT experiment since heat propagation is performed from the defect to the surface, whereas for optical techniques heat travels from the surface to the defects and back to the surface. Hence, VT is very fast, even faster than PT. A typical experiment last from a fraction of a second to several seconds. In addition, the longer the transducer operates at the surface; the most heat is released at the contact surface, increasing the probability of damaging the area. Furthermore, the pressure applied between the horn and the specimen has a great impact on the thermal response [41].

4.3. Processing vibrothermography data

Although raw thermograms present sometimes good enough contrast to detect defects, some processing is required most of the time. As for the case of LT and PT, the FFT algorithm can used and amplitude and phase images are recovered through Eqs. (7) and (8).

4.4. Advantages, disadvantages and applications

In either lock-in or burst configuration, VT is extremely fast, although it is necessary to relocate the transducer (and to immobilize the specimen again) to cover a large area for inspection. Hence, VT is more suitable for relatively small objects. It is the most appropriate technique to inspect some types of defects, *e.g.* micro cracks. On the contrary, it does not perform very well in some other cases in which application of optical techniques are straightforward, *e.g.* water detection. But probably the most inconvenient aspect of VT is the need of a coupling media between the sample and the transducer, and the need of holding the specimen. On the other hand, there is only minimal heating of the inspected specimen since energy is usually dissipated mostly at the defective areas, although there is some localized heating at the coupling and clamping points.

5. Comparative results

A CFRP panel, shown Figure 12, was inspected by the tree active techniques described above. The panel consists of a honeycomb core of 1.6 cm between two 10-ply CFRP. Several Teflon® inserts of different dimensions and thickness as specified in the figure are placed at different locations and depths. The group of defects at the top (defects 1 to 20) are analyzed first. It is possible to detect almost all of the defects by PPT as can be seen from Figure 13a and b.

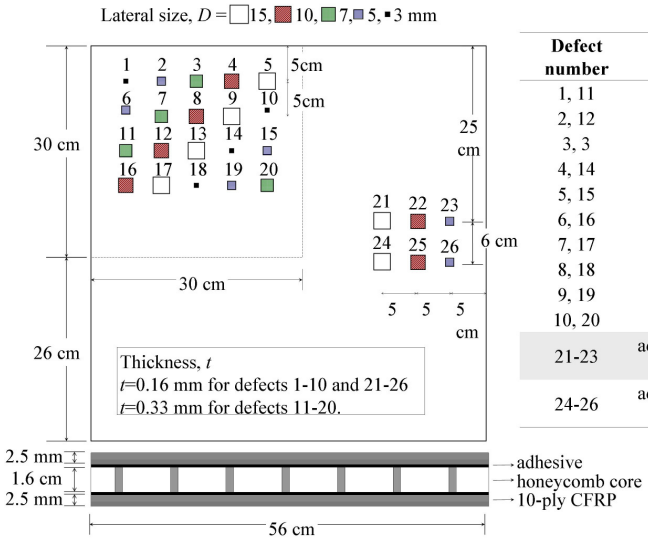

Defect number	Between plies
1, 11	1-2
2, 12	2-3
3, 3	3-4
4, 14	4-5
5, 15	5-6
6, 16	6-7
7, 17	7-8
8, 18	8-9
9, 19	9-10
10, 20	9-10
21-23	adhesive and core
24-26	adhesive and CFRP

Figure 12. Specimen HONEYCOMB 1108.

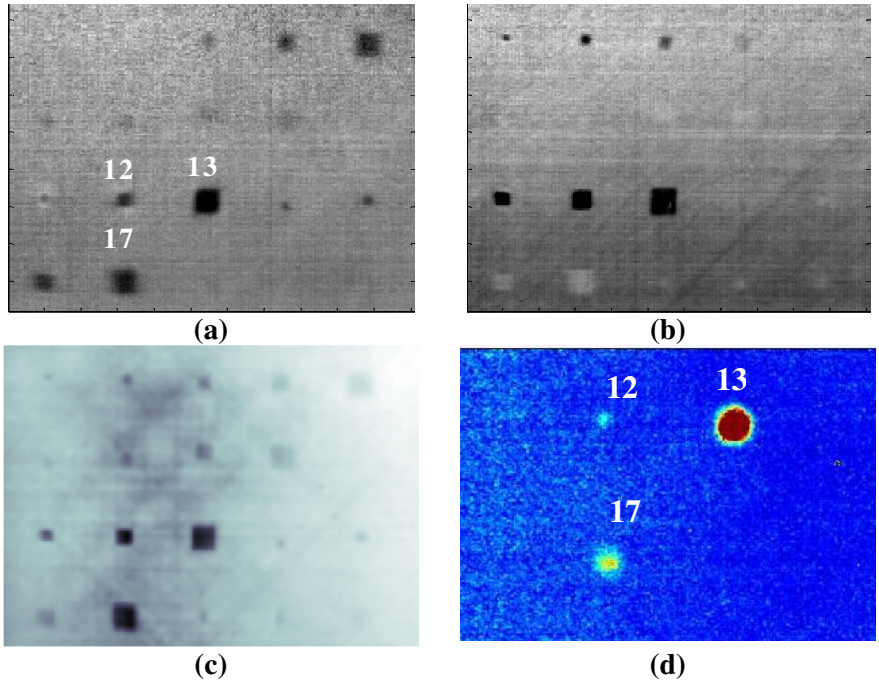

Figure 13. Comparative results for specimen HONEYCOMB 1108. shallowest group of defects. Synthetic PPT phase from a 7th degree polynomial at f =(a) 0.082 and (b) 0.74 Hz, (c) LT phase at f =0.001 Hz, and (d) VT result.

Contrast is better for shallower defects, although better results could be obtained for deeper defects using longer acquisition times using the same time resolution. The LT phasegram at f=0.001 Hz is presented in Figure 13c. Compared to PPT results, contrast is better for most of the defects and worse for a few others, but with the exception of defect number 10, all defects can be seen in a single phasegram. On the other hand, only the thicker (L=0.33 mm) inserts could be detected by VT. Defect number 12 is 0.5 mm deep and 10 mm large, defect 13 is 0.75 mm deep and 15 mm large, whilst defect 17 is 1.75 mm deep and 15 mm large.

Results for the deepest set of inserts (defects 21 to 26) are seen in Figure 14. While only assumptions of the location of these defect can be made from PT and LT results (Figure 14a and b, respectively), amplitude and phase images by VT (Figure 14c and d, respectively) clearly show the presence of the two largest defects (defects number 21 and 24 in Figure 12).

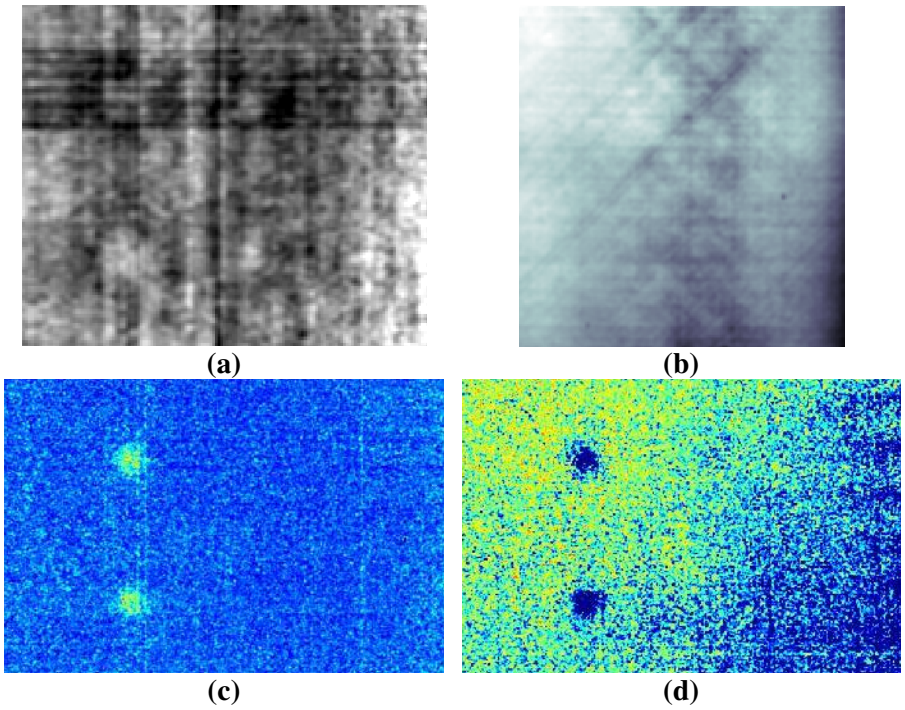

Figure 14. Comparative results for specimen HONEYCOMB 1108. deepest group of inserts. (a) PPT phase at f = 0.041 Hz, (b) LT phase at f =0.001 Hz, and second frequency components for the (c) amplitude and (d) phase data by VT.

Only the two largest defects can be detected by VT. This is due probably to the way the inserts where positioned during the fabrication process. The

transition from the carbon-epoxy matrix to Teflon® is much less dramatic than the one from carbon-epoxy to air. Hence, probably in the case of the largest defects, there was more air trapped between the inserts and the glue promoting the dissipation of heat in the area. For the VT experiment, the IR camera was recording from the side with the inserts and the transducer was placed on the same side. Thermal waves only had to travel the distance from the location of the defects to the surface, while for the case of LT and PT, the thermal excitation came from the same side where data was collected, *i.e.* the thermal waves had to travel twice the distance when compared to VT.

6. Conclusions

The three main active thermography techniques can be used in the NDT assessment of materials and structures in many areas. Lock-in thermography allows having a better control of the energy that is to be deposited on a surface. This is of critical importance for the inspection of delicate specimens such as cultural properties and works of art. In addition, defect characterization (depth retrieval, determination of thermal properties) is straightforward from the diffusion length equation. Lock-in thermography however, requires performing several experiments to completely cover the range of depths.

Pulsed thermography is faster and easier to deploy, although experiments are performed having less control over the injected energy. Raw data is commonly affected by problems such as uneven heating, emissivity variations, reflections from the environment and surface geometry sharp variations. Nevertheless, a wide variety of processing techniques are available, which allows not only carrying out qualitative but also quantitative inspections.

The vibrothermography approach is relatively new on the active thermography scene. It had showed however to be very attractive for the inspection of some types of defects. For instance, it is possible to detect deeper defects by vibrothermogrpahy than with optical means. This is because of the way heat is generated and transformed into heat. In VT, the thermal waves only have to travel half the distance (from the defect to the surface) than with optical methods (from the surface to the defect and back). Nevertheless, VT is still lacking of quantitative studies, and very often optimal inspection parameters must be found experimentally.

In summary, a group of active techniques is available for a wide variety of applications. The selection of the most adequate approach depends on the particular application and the available experimental and expertise resources.

References

[1] Maldague X. P. V., Streckert H. H and Trimm M. W. "Introduction to infrared and thermal testing: Part 1. Nondestructive testing," in Nondestructive Handbook, Infrared and Thermal Testing, Volume 3, X. Maldague technical ed., P. O. Moore ed., 3rd edition, Columbus, Ohio, ASNT Press, 2001, 718 p.

[2] Giorleo G. and Meola C. "Comparison between pulsed and modulated thermography in glass-epoxy laminates", *NDT&E International*, **35**:287–292, 2002.

[3] Nordal P. E. and Kanstand S. O. "Photothermal radiometry," *Physica Scripta*, **20**:659-662, 1979.

[4] Busse G. "Techniques of infrared thermography: Part 4. Lockin thermography," in Nondestructive Handbook, Infrared and Thermal Testing, Volume 3, X. Maldague technical ed., P. O. Moore ed., 3rd edition, Columbus, Ohio, ASNT Press, 2001, 718 p.

[5] Wu D. and Busse G. "Lock-in Thermography for NonDestructive Evaluation of Materials," *Rev. Gén. Therm*., **37**:693-703, 1998.

[6] Carslaw H. S. and Jaeger J. C. *Conduction of Heat in Solids*, 2nd edition, Clarendon Press, Oxford, 1986.

[7] Favro L. D. and Han X. "Thermal Wave Materials Characterization and Thermal Wave Imaging," in Birnbaum G., Auld B. A. (eds.): *Sensing for Materials Characterization, Processing and Manufacuring*, ASNT TONES, **1**:399-415, 1998.

[8] Busse G., Wu D. and Karpen W. "Thermal Wave Imaging with Phase Sensitive Modulated Thermography," *J. Appl. Phys.*, **71**(8):3962-3965, 1992.

[9] Krapez J. C. "Compared performances of four algorithms used for modulation thermography", *Proc. 4th Conference on Quantitative InfraRed Thermography - QIRT*, D. Balageas, G. Busse, C. Carlomagno (eds.), Eurotherm Seminar 60, Lodz, Pologne, September 7-10, 1998, 148-153.

[10] Maldague X. P. and Marinetti S. "Pulse Phase Infrared Thermography," *J. Appl. Phys.*, **79**(5):2694-2698, 1996.

[11] Bracewell R. The Fourier Transform and its Applications, McGraw-Hill, USA, 1965.

[12] Cooley J. W. and Tukey J. W. "An Algorithm for the Machine Calculation of Complex Fourier Series," *Mathematics of Computation*, **19**(90):297-301, 1965.

[13] Busse G. and Rosencwaig A. "Subsurface Imaging with Photoacoustics," *Appl. Phys. Lett*., **36**(10):815-816, 1980.

[14] Meola C., Carlomagno G. M. and Giorleo G. "The Use of Infrared Thermography for Materials Characterization", *J. Mater. Process. Technol.*, **155-156**:1132–1137, 2004.

[15] Meola C. and Carlomagno G. M. "Recent Advances in the Use of Infrared Thermography", *Meas. Sci. Technol.*, **15**:27–58, 2004.

[16] Bai W. and Wong B. S. "Evaluation of Defects in Composite Plates under Convective Environments using Lock-In Thermography," *Meas. Sci. Technol.*, **12**:142-150, 2001.

[17] Busse G. "Nondestructive Evaluation of Polymer Materials," *NDT&E Int.*, **27**(5):253-262, 1994.

[18] Thomas R. L., Pouch J. J., Wong Y. H., Favro L. D. and Kuo P. K. "Subsurface Flaw Detection in Metals by Photoacustic Microscopy", *J. Appl. Phys*., **51**(2): 1152–1156, 1980.

[19] Carlomagno G. M. and Meola C. "Comparison between thermographic techniques for frescoes NDT", *NDT&E International*, **35**:559–565, 2002.

[20] Ibarra-Castanedo C., Bendada A. and Maldague X. "Image and signal processing techniques in pulsed thermography," *GESTS Int'l Trans. Computer Science and Engr.,* **22**(1): 89-100, November 2005.

[21] Ibarra-Castanedo C., González D., Klein M. Pilla M., Vallerand S. and Maldague X.

"Infrared Image Processing and Data Analysis," *Infrared Phys. Technol*., **46**(1-2):75-83, 2004.

[22] Maldague X. P. V., Theory and Practice of Infrared Technology for NonDestructive Testing, John Wiley-Interscience, 684 p., 2001.

[23] Martin R. E., Gyekenyesi A. L., Shepard S. M., "Interpreting the Results of Pulsed Thermography Data," Materials Evaluation, **61**(5):611-616, 2003.

[24] Pilla M., Klein M., Maldague X. and Salerno A., "New Absolute Contrast for Pulsed Thermography," QIRT 2002, D. Balageas, G. Busse, G. Carlomagno (eds.), *Proc. of QIRT*, pp. 53-58, 2002.

[25] Pilla M. "A Novel Contrast Method for Pulse Thermography Data", *Ph.D. Thesis*, Politecnico di Milano, 2002.

[26] Klein M., Pilla M. and Maldague X. "IR_View: A graphical user interface to process infrared images with MATLAB," application and documentation available online [http://irview.m-klein.com].

[27] González D. A., Ibarra-Castanedo C., Pilla M., Klein M., López-Higuera J. M. and Maldague X., "Automatic Interpolated Differentiated Absolute Contrast Algorithm for the Analysis of Pulsed Thermographic Sequence," *Proc. 7th Conference on Quantitative InfraRed Thermography (QIRT)*, Rhode Saint Genèse, Belgium, July 5-8, 2004, H.16.1-H.16.6.

[28] Benítez H. D., Ibarra-Castanedo C., Bendada A., Maldague X. and Loaiza H. "Modified Differential Absolute Contrast Using Thermal Quadrupoles for the Nondestructive Testing of Finite Thickness Specimens by Infrared Thermography," *Proc. CCECE 2006 - Canadian Conference on Electrical and Computer Engineering,* Ottawa (Ontario) Canada, May 7-10, 2006, Paper No. **398**.

[29] Ibarra-Castanedo C. and Maldague X. "Pulsed Phase Thermography Reviewed," *QIRT J.*, **1**(1):47-70, 2004.

[30] Ibarra-Castanedo C. "Quantitative subsurface defect evaluation by pulsed phase thermography: depth retrieval with the phase," *Ph. D. thesis*, Laval University, 2005. [accessible online: http://www.theses.ulaval.ca/2005/23016/23016.pdf].

[31] Galmiche F., Vallerand S. and Maldague X. "Pulsed phase thermography with the wavelet transform," in Review of progress in Quantitative NDE, D. O. Thompson and D.E. Chimenti (eds.), American Institute of Physics, **19A**:609-615, 2000.

[32] Ibarra-Castanedo C., González D. A., Galmiche F., Bendada A. and Maldague X. "Chapter 5 : On signal transforms applied to pulsed thermography," *Recent Res. Devel. Applied Phys.*, **9**(2006):101-127, 2006.

[33] Shepard S. M. "Advances in Pulsed Thermography", *Proc. SPIE - The International Society for Optical Engineering, Thermosense XXVIII*, Orlando, FL, 2001, Eds. A. E. Rozlosnik and R. B. Dinwiddie, **4360**:511-515, 2001.

[34] Ibarra-Castanedo C. and Maldague X. "Interactive methodology for optimized defect characterization by quantitative pulsed phase thermography," *Research in Nondestructive Evaluation,* **16**(4):1-19, 2005.

[35] Dillenz A., Zweschper T. and Busse G. "Progress in ultrasound phase thermography," *Proc. SPIE - The International Society for Optical Engineering, Thermosense XXVIII*, Orlando, FL, 2001, Eds. A. E. Rozlosnik and R. B. Dinwiddie, **4360**:574-579.

[36] Favro L. D., Han X., Ouyang Z., Sun G., Sui H. and Thomas R. L. "Infrared imaging of defects heated by a sonic pulse," *Rev. Sci. Instr.*, 2000.

[37] Busse G. "Optoacoustic and photothermal material inspection techniques," *Applied Optics*, **21**(1):107-110, 1982.

[38] Thomas R. L. "Thermal NDE techniques – from photoacoustics to thermosonics," *Review of Quantitative Nondestructive Evaluation*, Eds. D. O. Thompson and D. E. Chimenti, **21**:3-13, 2002.

[39] Sinha S. K., Iyer S. R. and Bhardwaj M. C. "Non-contact ultrasonic sensor and state-of-the-art camera for automated pipe inspection," *Proceedings of IEEE Sensors*, **2**(1):493-498, 2003.

[40] Zweschper T., Riegert G., Dillenz A. and Busse G. "Frequency modulated elastic wave thermography," *Proc. SPIE - The International Society for Optical Engineering, Thermosense XXV*, Orlando, FL, 2003, Eds. K. E. Cramer and X. P. Maldague, **5073**:386-391.

[41] Shepard S. M., Ahmed T. and Lhota J. R. "Experimental considerations in vibrothermography," *Proc. SPIE - The International Society for Optical Engineering, Thermosense XXVI*, Orlando, FL, 2004, Eds. D. D. Burleigh, K. E. Cramer and G. R. Peacock, **5405**:332-335.